Preparation, Characterization, and Thermal Properties of Controllable Metal–Imidazole Complex Curing Agents for Epoxy Resins

JULIE BROWN, IAN HAMERTON, BRENDAN J. HOWLIN

Department of Chemistry, School of Physics and Chemistry, University of Surrey, Guildford, GU2 5XH, United Kingdom

Received 9 June 1998; accepted 4 April 1999

ABSTRACT: A series of complexes incorporating the epoxy–imidazole adduct of phenyl glycidyl ether with 2-ethyl-4-methylimidazole (PGE-EMI), has been prepared with the acetato and chloro transition metal salts of Mn, Co, Ni, Cu, Zn, and Ag. These complexes have been characterized using spectroscopic methods (IR, UV-Vis, ^{1}H- and ^{13}C-NMR, where appropriate) and their thermal stabilities have been determined using elevated temperature NMR techniques. These high-temperature NMR results indicated that the chloro complexes studied (of Mn^{2+}, Co^{2+}, Ni^{2+}, Cu^{2+}, and Zn^{2+}) exist in equilibrium (i.e., they dissociate reversibly in a solution of dimethylsulphoxide, DMSO, at elevated temperatures), while the corresponding acetato complexes dissociate irreversibly. For the silver complexes, thermogravimetric analysis (TGA) was used to monitor the dissociation, showing that the weight loss recorded was consistent with the dissociation of the metal salt to liberate the PGE–imidazole ligand. The thermal stabilities of the metal complexes were influenced by changing both the transition metal (e.g., from Mn to Zn) and varying the anion (e.g., from acetate to chloride). From ^{1}H-NMR analysis, a decrease of ca. 10°C was observed in the thermal dissociation of the acetato complexes when compared with the chloro complexes, showing that the series of PGE-EMI complexes with acetate anions is less thermally stable than the corresponding chlorides. This finding suggests that these PGE-EMI complexes may be modified to accommodate their use in a variety of different curing schedules when used to cure epoxy resins. © 2000 John Wiley & Sons, Inc. J Appl Polym Sci 75: 201–217, 2000

Key words: epoxy; curing agent; latent cure; cure kinetics; imidazoles

INTRODUCTION

It is well established that imidazoles will complex with many metal salts in the Periodic Table; the most studied being those of the *d*-block transition metals. Imidazole complexes are capable of initiating the homopolymerization of epoxide groups via a polyetherification reaction, and the reaction of difunctional epoxies in this way leads to the formation of polymer networks.[1] Furthermore, the introduction of metal–imidazole complexes into polymer matrices has been shown to improve some properties of epoxy resin systems. For example, increases in mechanical properties (e.g., tensile strength) and electrical properties (e.g., dielectric constant) have been observed,[2] and polymers that have been modified in this way have been shown to have higher thermo-oxidative and chemical resistance.[3]

While early (solid) imidazole complexes exhibited high storage stability in the presence of epoxy resins at room temperature over uncomplexed

Correspondence to: I. Hamerton.

Contract grant sponsors: The Cookson Technology Group, Yarnton.

Journal of Applied Polymer Science, Vol. 75, 201–217 (2000)

 CCC 0021-8995/00/020201-17

imidazoles,[4] a major drawback was their poor solubility when mixed with epoxies. This was due to the irregular dispersion of the solid particles throughout the epoxy matrix, leading to the complexes settling out on storage. The addition of a phenyl glycidyl ether (PGE) group to the imidazole via a substitution reaction increased the solubility of these metal complexes in both epoxy oligomers and organic solvents.[5] Furthermore, complexation of a 1 : 1 adduct of PGE and 2-ethyl-4-methylimidazole (EMI) (namely PGE-EMI) with a variety of transition metal salts has been shown to be effective in producing curing agents for use at elevated temperatures.[5] These complexes, one such example being $Cu(PGE\text{-}EMI)_4Cl_2$, can act as latent curing agents exhibiting improved storage stability when compared with either the simple imidazoles (containing no PGE), or the uncomplexed PGE-EMI ligand. This is a direct result of coordinating both pyridine, N(3) and pyrrole, N(1) nitrogen atoms, thereby reducing their reactivity at room temperature (see Fig. 1).

On heating, these PGE-EMI–based complexes dissociate to liberate the free PGE-EMI ligand, allowing it to interact with the epoxy groups and initiate cure[6] (Fig. 2). Some complexes have been shown to undergo dissociation at elevated temperatures, allowing the adduct to initiate cure, but when cooled, the complex has been observed to reassociate.[6a] In an earlier study Poncipe[7] prepared a series of complexes of the form $M(PGE\text{-}EMI)_4Cl_2$ (where M = Co, Ni, and Cu). He also studied the temperature dependence of these complexes in solution using UV spectroscopic techniques to determine their thermal stability behaviour; the Cu^{2+} complex was found to be the most thermally stable. Subsequent studies[6,8] have further highlighted the application of these (PGE-EMI)–metal complexes as effective curing agents for epoxy resins. For example, upon the application of heat, $Cu(PGE\text{-}EMI)_4Cl_2$ (6a) dissociates reversibly to liberate the free imidazole ligand, which initiates cure in the epoxy system. Initially, Poncipe's work was repeated to obtain a spectroscopic characterization for the chloro complex. These data were used as a preliminary study leading to the development of a series of novel metal–acetato complexes of the form $M(PGE\text{-}EMI)_4(CH_3COO^-)_2$. This study will allow us to (1) ascertain whether other transition metals (Mn, Co, Ni, and Zn) will behave in a similar fashion to Cu, and (2) investigate the effect of changing both the transition metal and the anion upon the stereochemistry of the desired complexes, leading to a series of thermal dissociation temperatures to be employed in different cure schedules.

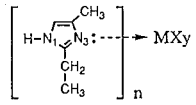

(a)

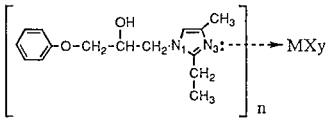

(b)

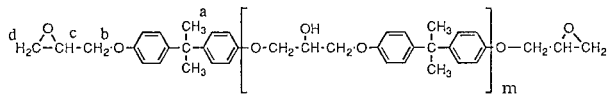

(Epikote 828 oligomer)

Figure 1 Structures of the compounds employed in this study (with ^{1}H-NMR designations). (a) Simple metal–imidazole and (b) (PGE-EMI)–metal complexes, where n = number of imidazole ligands to be coordinated, M = metal cation, X = anion, y = number of anion ligands, m = degree of polymerization.

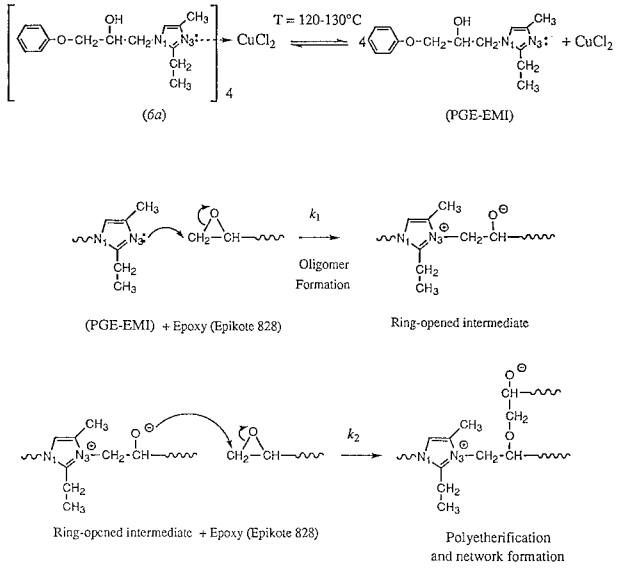

Figure 2 Scheme for the thermal dissociation of the complexes, adduct formation, and polyetherification of a commercial epoxy resin.

We report here the preparation and characterization of a series of complexes incorporating the PGE-EMI ligand, with the acetato and chloro transition metal salts of Mn, Co, Ni, Cu, Zn, and Ag. High-temperature nuclear magnetic resonance (NMR) spectroscopic results indicated that the chloro complexes studied (of Mn^{2+}, Co^{2+}, Ni^{2+}, Cu^{2+}, and Zn^{2+}) exist in equilibrium (i.e., they dissociate reversibly in a solution of DMSO, at elevated temperatures), while the corresponding acetato complexes dissociate irreversibly. Thermogravimetric analysis (TGA) results for the silver complexes showed that the weight loss recorded was consistent with the dissociation of the metal salt to liberate the PGE-EMI ligand.

The thermal stabilities of the metal complexes were influenced by changing both the transition metal (e.g., from Mn to Zn) and varying the anion (e.g., from acetate to chloride, suggesting that these PGE-EMI complexes may be modified to accommodate their use in a variety of different curing schedules when used to cure epoxy resins. However, the true efficiency of these complexes as curing agents will only be apparent in studies with commercial epoxy resins, and in this article we address kinetic aspects of the cure process.

EXPERIMENTAL

Materials

Phenyl glycidyl ether (PGE) and 2-ethyl-4-methylimidazole (EMI) were obtained from Aldrich Chemical Company, and their purities assessed using ^{1}H-NMR spectroscopy. Metal(II) acetates and chlorides were obtained from BDH and Aldrich, respectively, and were available in their hydrated form. Silver(I) salts of acetate and nitrate were obtained from Aldrich, and gave acceptable analytical results (Table I). This table also gives the designation for each complex that is used throughout this article. Analytical data for the complexes are presented therein.

Analytical Techniques

^{13}C-Nuclear magnetic resonance (NMR) spectra of the complexes were obtained in d_6-DMSO and $CDCl_3$, where appropriate, at 25°C using a Bruker AC-300E Spectrometer operating at 300.13 and 75.46 MHz, respectively. All ^{1}H-NMR chemical shift (δ) are reported in ppm relative to an internal tetramethylsilane (TMS) standard, ^{13}C-NMR spectra are referenced to the particular solvent used ($CDCl_3$ or d_6-DMSO).

Variable temperature ^{1}H-NMR spectroscopy (VT-NMR) of the $M(PGE\text{-}EMI)_4(CH_3COO^-)_2$ and $M(PGE\text{-}EMI)_4Cl_2$ series, where M = Mn, Co, Ni, and Cu, were obtained in d_6-DMSO, using a Bruker AC-300E Spectrometer operating at 300.13 MHz at varying temperatures; all chemical shifts are reported in ppm relative to an internal 1,4-dimethoxybenzene standard.

Infrared (IR) spectra of all complexes were obtained as Nujol mulls or thin films on KBr plates, where appropriate, in the region of 4000–370 cm^{-1} using a Perkin-Elmer System 2000 FTIR spectrometer interfaced with a Perkin-Elmer computer and an ATI Mattson Research Series FTIR spectrometer as Nujol mulls or thin films on CsI plates in the region of 600–200 cm^{-1}.

UV-Visible spectra of all complexes were obtained using a Perkin-Elmer 306 UV-VIS spectrophotometer, using a quartz cell of path length 1 cm. The reference solvents were methanol, dichloromethane, and ethanol where appropriate, and samples were scanned in the region of 270–900 nm.

Thermal dissociation of the $Ag(PGE\text{-}EMI)_2X$ complexes, where X = NO_3 or acetate, was studied using a Shimadzu TA501 thermal analyzer interfaced with a Shimadzu computer operating system. The operating conditions were sample rate of 10 K min^{-1} under N_2 (40 cm^3 min^{-1}) using aluminum pans following a temperature ramp from room temperature to 490°C.

Elemental (C, H, N) microanalyses of all complexes were obtained using a Leemans Labs 440 elemental analyzer.

Atomic absorption spectra (AAS) of manganese, cobalt, nickel, and copper were obtained using a Perkin-Elmer 306 atomic absorption spectrometer operating at wavelengths of 279.5 (for Mn), 240.7 (Co), 232.0 (Ni), and 324.7 nm (Cu), a slit setting of 4, and using a hollow cathode lamp and air/acetylene flame. The acetates of manganese, cobalt, and nickel were used as the standards in solvent compositions of 80 : 20 (v/v) water/ethanol mixtures, while copper^{2+} acetate was studied in 96% ethanol only. Silver and zinc analyses were carried out on the same instrument, but using wavelengths of 328.0, 213.9 nm, respectively. Silver^{1+} nitrate and acetate and zinc^{2+} chloride and acetate, were used as the standards in 50 : 50 (v/v) methanol/water solvent compositions.

Table I Analytical Data for Complexes Prepared in This Work

Metal Salt	Complex Designation	Ligand[a]	Metal : Ligand Ratio	Empirical Formula of Complex	Elemental Analysis (%)[b] C	H	N	M	Yield (%)	Appearance
$MnCl_2$	1a	EMI	1 : 3	$[MnCl_2(EMI)_3]$	47.68	6.72	18.48	12.26	66.3	Brown solid
					(47.36	6.63	18.41	12.04)		
$Mn(CH_3COO^-)_2$	1b	EMI	1 : 1	$[Mn_2(CH_3COO^-)_2(EMI)_2] \cdot 4H_2O$	37.78	5.35	11.05	24.51	27.8	Dark brown solid
					(37.51	5.13	10.94	24.49)		
$MnCl_2$	1c	PGE-EMI	1 : 3	$[MnCl_2(PGE\text{-}EMI)_3] \cdot 3H_2O$	56.01	6.87	8.70	5.71	41.2	Brown viscous oil
					(56.23	6.94	8.75	5.72)		
$Mn(CH_3COO^-)_2$	1d	PGE-EMI	1 : 1	$[Mn_2(CH_3COO^-)_2(PGE\text{-}EMI)_2] \cdot 4H_2O$	48.25	6.05	6.07	4.56	18.4	Dark brown solid
					(48.65	6.45	5.97	4.56)		
$CoCl_2$	2a	EMI	1 : 4	$[Co(EMI)_4Cl_2] \cdot 4H_2O$	44.69	7.62	17.35	9.00	59.8	Royal-blue solid
					(44.85	7.54	17.44	9.11)		
$Co(CH_3COO^-)_2$	2b	EMI	1 : 4[c]	$[Co(CH_3COO^-)_2(EMI)_4] \cdot C_2H_5OH$	54.00	7.86	16.72	8.80	46.1	Purple oil
					(54.28	7.91	16.88	8.88)		
$CoCl_2$	2c	PGE-EMI	1 : 4	$[Co(PGE\text{-}EMI)_4Cl_2] \cdot 4H_2O$	54.49	6.39	8.39	4.44	35.2	Royal-blue solid
					(54.61	6.43	8.49	4.74)		
$Co(CH_3COO^-)_2$	2d	PGE-EMI	1 : 4	$[Co(CH_3COO^-)_2(PGE\text{-}EMI)_4] \cdot 4H_2O$	59.27	7.35	8.68	4.57	53.8	Purple oil
					(59.56	7.30	8.58	4.57)		
$NiCl_2$	3a	EMI	1 : 4	$[Ni(EMI)_4Cl_2] \cdot 4H_2O$	44.93	7.49	17.41	9.10	46.3	Green solid
					(44.86	7.55	17.44	9.14)		
$Ni(CH_3COO^-)_2$	3b	EMI	1 : 2	$[Ni(CH_3COO^-)_2(EMI)_2] \cdot 4H_2O$	40.62	7.28	11.87	12.36	43.1	Green solid
					(40.95	7.32	11.94	12.51)		
$NiCl_2$	3c	PGE-EMI	1 : 2	$[NiCl_2(PGE\text{-}EMI)_2] \cdot 2H_2O$	52.53	6.43	8.23	8.53	89.5	Pink/purple glass
					(52.48	6.47	8.16	8.55)		
$Ni(CH_3COO^-)_2$	3d	PGE-EMI	1 : 4	$[Ni(CH_3COO^-)_2(PGE\text{-}EMI)_4] \cdot 4H_2O$	60.03	7.44	8.80	4.72	53.8	Dark green glass
					(59.57	7.04	8.69	4.55)		
$ZnCl_2$	4a	EMI	1 : 4	$[Zn(EMI)_4Cl_2] \cdot 4H_2O$	44.53	7.49	17.39	10.07	17.5	White crystals
					(44.40	7.47	17.27	10.07)		
$ZnCl_2$	4b	PGE-EMI	1 : 4	$[Zn(PGE\text{-}EMI)_4Cl_2] \cdot 4H_2O$	59.27	6.90	9.17	5.45	60.8	Straw-coloured solid
					(59.36	6.99	9.23	5.39)		
$Zn(CH_3COO^-)_2$	4c	PGE-EMI	1 : 2	$[Zn(CH_3COO^-)_2(PGE\text{-}EMI)_2] \cdot 2H_2O$	53.00	6.62	7.36	9.00	12.6	Straw-coloured solid
					(52.60	6.51	7.22	8.83)		
$AgNO_3$	5a	EMI	1 : 2	$[AgNO_3(EMI)_2]$	37.20	5.21	17.80	27.69	45.4	White solid
					(36.93	5.18	17.95	27.63)		
$AgNO_3$	5b	PGE-EMI	1 : 2	$[AgNO_3(PGE\text{-}EMI)_2]$	51.88	5.94	10.11	15.57	71.9	Brown glass
					(52.17	5.85	10.14	15.62)		
$Ag(CH_3COO^-)$	5c	PGE-EMI	1 : 2	$[Ag(CH_3COO^-)(PGE\text{-}EMI)_2]$	56.01	6.41	8.12	15.69	74.5	Brown glass
					(55.89	6.32	8.15	15.69)		
$CuCl_2$	6a	PGE-EMI	1 : 4.5	$[CuCl_2(PGE\text{-}EMI)_4] \cdot 4H_2O$	58.04	7.08	8.96	5.00	48.1	Dark green

$Cu(NO_3)_2$	6b	PGE-EMI	1 : 4.5	$[Cu(NO_3)_2(PGE\text{-}EMI)_4] \cdot 4H_2O$	(57.74) 55.50 (55.38)	7.12 6.90 6.83	8.98 10.69 10.77	5.09) 4.89 4.88)	84.8	glass Dark green glass
$Cu(CH_3COO^-)_2$	6c	PGE-EMI	1 : 1	$[Cu_2(CH_3COO^-)_4(PGE\text{-}EMI)] \cdot 2H_2O$	36.29 (36.33	4.65 4.73	2.69 2.74	13.00 12.40)	51.0	Green solid
$Cu(CH_3COO^-)_2$	6d	PGE-EMI	1 : 2	$[Cu_2(CH_3COO^-)_4(PGE\text{-}EMI)_2] \cdot 2H_2O$	48.01 (47.70	5.85 5.93	4.79 4.84	11.00 10.97)	69.6	Blue solid
$Cu(CH_3COO^-)_2$	6e	PGE-EMI	1 : 4	$[Cu(CH_3COO^-)_2(PGE\text{-}EMI)_4]$	63.14 (62.84	7.25 7.10	9.42 9.16	5.65 5.20)	34.8	Blue/green oil

All complexes are isolated in a variety of hydrated forms.
[a] EMI, 2-ethyl-4-methylimidazole, PGE-EMI, 1,2-epoxy-3-propane-2-ethyl-4-methylimidazole.
[b] Calculated values are in parentheses.
[c] Complex precipitates with one molecule of ethanol.

Preparative Methods for the 2-Ethyl-4-Methylimidazole (EMI)–Metal Complexes

An earlier patent[5] concerning the preliminary work contained no details on the characterization of these complexes. Therefore, a full account of the preparation and analysis of these complexes is given below. The metal–imidazole complexes in the current work were all prepared using the same general method (i.e., complexation in ethanolic solution), except for silver and zinc, which were best suited to a methanol–water solvent system. The analytical data for these complexes are given in Table I.

Preparation of Complexes of the Type $M(EMI)_4X_2$, where M = Mn, Co, Ni; X = CH_3COO^-, Cl^-

To an ethanolic solution of EMI (0.04 mol) was added dropwise a solution of the metal salt (0.01 mol) in ethanol (10 cm^3). The mixture was stirred for 30 min, after which the solution was concentrated to ca. 5 cm^3 and precipitated with diethylether (20 cm^3), to yield highly colored solids. The Co^{2+} complexes were royal blue and purple (λ_{max} = 667, 524 nm); the Ni^{2+} complexes were green (λ_{max} = 667, 692, 732 and 749 nm) and Mn^{2+} complexes were brown. These solids were washed with a 2 : 1 (v/v) mixture of ether/ethanol (10 cm^3) and dried *in vacuo* at 50°C overnight.

Preparations of $Zn(EMI)_4Cl_2$, and $Ag(EMI)_2NO_3$ Metal Complexes

To a methanolic solution of EMI (0.02 and 0.04 mol) was added dropwise a solution of the metal salt in distilled water (10 cm^3). White precipitates were formed immediately, filtered, washed with methanol–water (20 cm^3) and dried *in vacuo* at 60°C overnight to yield white solids.

Preparation of the PGE-EMI Ligand

To a refluxing, stirred solution of EMI (27.5 g, 0.25 mol) in toluene (50 cm^3) was added dropwise over the course of 1 h, PGE (37.5 g, 0.25 mol) in toluene (50 cm^3). During this addition the solution turned from pale yellow to orange. The solution was further refluxed for ca. 2 h and decolorized with charcoal (1 g). The crude orange product was precipitated from solution by the addition of petroleum ether 40–60°C (100 cm^3) to yield a viscous orange product (yield 51.95 g, 79.5%). Purification of the PGE-EMI ligand was achieved using column chromatography, using a silica sta-

tionary phase and a 4 : 1 (v/v) chloroform/methanol mixture as the eluent. A single spot was observed at $R_f = 0.6$ using UV light at a wavelength of 254 nm.

Preparation of the (PGE-EMI)–Metal Complexes

Preparation of the M(PGE-EMI)$_4$X$_2$ Complexes Where M = Mn, Co, Ni, Cu, and X = Cl$^-$, CH$_3$COO$^-$

To a solution of the metal salt (0.01 mol) in ethanol was added a solution of PGE-EMI (0.04 mol) in ethanol (5 cm^3). The solution was stirred and gently heated for 30 min, after which the cooled solution was gravity filtered and concentrated to ca. 2 cm^3. The solution was precipitated using diethyl ether (5 cm^3), washed with a 2 : 1 mixture (v/v) of diethylether/ethanol (10 cm^3) and dried *in vacuo* at 50°C overnight to yield highly colored viscous oils. The Co^{2+} complexes were blue and purple (λ_{max} = 618.0, 565.1 nm); Ni^{2+} complexes were blue-purple and green (λ_{max} = 692, 684 nm) the Cu^{2+} complexes were dark green and blue (λ_{max} = 707.6, 675.3 nm) and the Mn^{2+} complexes were brown solids.

Preparation of Zn(PGE-EMI)$_4$Cl$_2$ and Zn(PGE-EMI)$_2$(CH$_3$COO$^-$)$_2$

To a methanolic solution of PGE-EMI (0.03 g, 3.03 $\times$ 10^{-5} mol) was added dropwise a solution of $ZnCl_2$ (4.13 $\times$ 10^{-3} g, 3.03 $\times$ 10^{-5} mol) in distilled water (1 cm^3). The solution was rapidly stirred for 30 min and no color changes were observed on addition of the Zn^{2+} salt. After 30 min, the solution was evaporated to dryness using rotary evaporation and dried for 24 hours *in vacuo* at 60°C to yield a straw-colored solid.

For the acetate complex, the same procedure was followed, but a metal : ligand ratio of 1 : 2 was used. The product obtained after drying *in vacuo* was a straw coloured solid.

Preparation of Ag(PGE-EMI)$_2$X, Where X = CH$_3$COO$^-$, NO$_3^-$

To a stirred solution of the PGE-EMI ligand (0.91 g, 1.74 $\times$ 10^{-3} mol) in methanol (5 cm^3) was added dropwise $AgNO_3$ (0.29 g, 1.74 $\times$ 10^{-3} mol) in distilled water (5 cm^3). The solution was stirred for 1 h, and a color change of orange to brown was noted. The complex was evaporated to dryness and dried *in vacuo* at 60°C overnight to yield a brown glass. A repeat procedure for the acetato complex was used, but the complex was further dried *in vacuo* at 100°C overnight and gave a brown glass.

Preparation of a Series of Copper Complexes of Type Cu(PGE-EMI)$_6$(CH$_3$COO$^-$)$_2$, Where y = 1 or 2

$Cu(CH_3COO^-)_2 \cdot H_2O$ (0.41 g, 2.05 $\times$ 10^{-3} mol) in ethanol (150 cm^3), was added dropwise to a stirred ethanolic solution of PGE-EMI (0.54 g, 2.05 $\times$ 10^{-3} mol). The solution turned blue and stirring was continued for 30 min. The blue solution was gravity filtered, and evaporated to dryness to yield a green solid of formula Cu(PGE-EMI)$(CH_3COO^-)_2$, which was filtered, washed with ethanol (10 cm^3), and dried *in vacuo* at 50°C overnight. For the 2 : 1 complex of formula $Cu(PGE\text{-}EMI)_2(CH_3COO^-)_2$, a blue solid was formed.

Preparation of Cu(PGE-EMI)$_4$(NO$_3$)$_2$

To a stirred solution of the PGE-EMI ligand (0.56 g, 4.73 $\times$ 10^{-4} mol) in ethanol (10 cm^3) was added dropwise $Cu(NO_3)_2 \cdot 4H_2O$ (0.12 g, 4.73 $\times$ 10^{-4} mol) in ethanol (5 cm^3). The solution was heated gently, and a color change (of yellow-orange to green) was observed. The solution was concentrated to ca. 5 cm^3, and the complex was precipitated by the addition of diethyl ether (10 cm^3). The complex was washed with a 2 : 1 mixture (v/v) of diethyl ether/ethanol (10 cm^3) and dried *in vacuo* at 60°C overnight to yield a brittle green glass.

RESULTS AND DISCUSSION

Preparation of the EMI–Metal and (PGE-EMI)–Metal Complexes

Table I details the physical data for the full range of complexes prepared during the course of this work. The nature of the metal, ligand, anion, and stoichiometry were all varied to examine the effect(s) of all features on the thermal (and ultimately epoxy cure) behavior. It is apparent that yields were variable, although only in a relatively few cases (1b, 1d, 4a and 4d) was the yield unacceptably low. From an examination of the appearance of the complexes, the majority of structures appear to exist with octahedral symmetry, the exceptions being 2a, 2c, and 3c, which appear to be tetrahedral complexes with chloride counter

anions. The microanalytical data are generally good, but show that in some cases unexpected complexes were produced (e.g., rather than the 1 : 4 metal : ligand ratio that was desired, $MnCl_2$ complexes 1a and 1c precipitate as 1 : 3 metal complexes; $Mn(CH_3COO^-)_2$ complexes 1b and 1d precipitate as 1 : 1 metal complexes; the $NiCl_2$ complex, 3c, precipitates as a 1 : 2 metal complex, and the $Co(CH_3COO^-)_2$ complex, 2b, precipitates with one molecule of ethanol).

Only a few of the metal$(EMI)_4Cl_2$ complexes have been reported previously in an earlier patent,[1] but no spectroscopic or analytical data were given, and so the current article represents the first systematic study of these materials. In related work,[4] these complexes were also used to cure a commercial epoxy (Epon 828®) based on bisphenol A diglycidyl ether (BADGE).

Barton[5] also prepared a range of modified imidazole complexes, including $Cu(PGE\text{-}EMI)_2(CH_3COO^-)_2$ and $Cu(PGE\text{-}EMI)_4(NO_3)_2$, to overcome the inherently poor solubility of transition metal–imidazole complexes when formulated with epoxy systems. The addition of the PGE moiety served to enhance the compatibility of the two components by making the curing agent resemble the backbone of the epoxy oligomer. Barton[5] used both complexes to cure another commercial BADGE-type epoxy (Epikote 828) and found that the process could be effected at different temperatures: the onset of cure occurring at either 80°C [$Cu(PGE\text{-}EMI)_2(CH_3COO^-)_2$] or 105°C [$Cu(PGE\text{-}EMI)_4(NO_3)_2$].

With the exception of the chloride and nitrate complexes of $M(PGE\text{-}EMI)_2X_4$ (M = Cu and Co), all of the compounds prepared are believed to be novel. The steric hindrance afforded by the PGE-EMI ligand, and its hygroscopic nature, make it difficult to obtain single crystals of the subsequent complexes.

NMR Data

^{13}C-NMR data are given in Tables II and III. As many of the ^1H-NMR spectra contained broad chemical shifts, it is difficult to assign the chemical shifts with confidence. For example, both the methyl (of the CH_3COO^-) and the methylene protons (of the EMI) overlap, leading to broadened signals around δ = 2.5 ppm. Furthermore, the presence of the d_6-DMSO signal (δ = 2.52 ppm) also tends to obscure the methylene protons (of the EMI). In common with observations made during our earlier work in this area,[6a] the imidazole ring protons are also shifted downfield in some cases after complexation, and are indistinguishable from the chemical shifts arising from the phenyl ring protons. It should be noted that Mn^{2+} complexes (1a and 1b) showed extremely broad signals due to the high paramagnetism of the complexes, making assignment ambiguous. From an examination of the imidazole structure (Fig. 1) it can be seen that there is the possibility of forming two distinct isomers between PGE and N(1) or N(3) atoms on the imidazole. The chemical environment of atoms in these two isomers are sufficiently different to give rise to unique chemical shifts. Consequently, in Table II, some chemical shift data are given for both isomers (e.g., in Table II, the ^{13}C shift for C(3) in complex 4b is given as both 114.02 and 114.50 ppm).

IR Data

Selected IR data for the metal–imidazole complexes are given in Table IV. In some cases, the occurrence of overlap between bands made positive assignment difficult. This is particularly apparent in the case of the C—N stretching vibration in Mn and Ni complexes (1b, 3b, and 3d), which is hidden by the symmetrical vibration of the acetato signal; the C—N deformation and the C═N stretch, which both coincide with the ionic nitrate band at 1384–1385 cm^{-1} and the antisymmetric stretch of the acetato ligand (affecting complexes 5a and 5c). Furthermore, the C—C skeletal stretching vibration of the benzene ring overlaps with the symmetric stretch of the acetato ligand (in complexes 1d, 4c, 5c, and 6e). It was noted that complex 3a displayed additional broad peaks at 3391–3392 cm^{-1} and 824 cm^{-1}, indicating the presence of lattice water.

To verify whether complexation had occurred, the complexes were analyzed using vibrational spectroscopy (in the far-IR region). The spectrum of the parent EMI ligand was quite complex, with numerous bands between 293 and 385 cm^{-1}, making full assignment difficult, but in common with data reported by Eilbeck et al.,[9] a strong band was observed at 262 cm^{-1}. We monitored the position of this band after complexation of the ligand with a variety of metals. It was apparent that in the case of the chlorides the following bands were observed for Metals = Mn (1a, 285 cm^{-1}), Co (2a, 337 cm^{-1}), Ni (3a, 279 cm^{-1}), and Zn (4a, 323 cm^{-1}).

Table II ^{13}C-NMR Shifts of Various Adducts and Complexes (Given as δ ppm Relative to TMS)

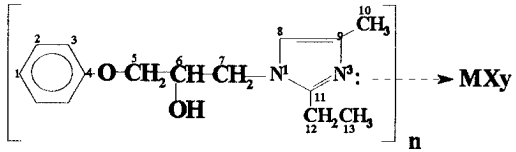

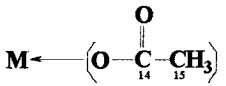

X = NO_3, acetate

Complex	C_1	C_2	C_3	C_4	C_5	C_6	C_7	C_8	C_9	C_{10}	C_{11}	C_{12}	C_{13}	C_{14}	C_{15}
4b	120.63	128.30	114.02	158.31	68.27	69.49	46.59	116.67	129.05	12.59	149.12	18.96	13.22	N/A	N/A
			114.50	158.22	68.46	69.27	48.07	122.44	134.01	9.44	150.66	19.29	12.72		
											ca.				
4c	120.64	129.59	114.54	158.30	68.39	69.29	46.54	116.66	129.01	12.58	150(b)	18.98	13.00	175.96	23.35
					68.49	69.48	48.14	122.97	13.04	9.49		19.33	12.68		
5b	121.15	129.53	114.41	158.07	68.05,	68.61,	47.73,	117.78	129.06,	13.42	150.95	20.87	13.42	N/A	N/A
					68.61	68.93	49.62	124.51	134.45	9.74	151.00	21.50	13.58		
5c	121.25	129.71	114.60	158.39	69.35	69.77	47.86	116.40	128.72	12.12	150.78	20.93	13.66	178	24.08
					69.51	69.98	49.75	123.95	134.71	10.11	151.34	21.41	14.51		
PGE-EMI	121.95	130.12	115.05	158.78	68.50	69.46	47.51	116.70	127.56	12.52	149.80	20.53	13.14	N/A	N/A
					68.97	69.69	49.31	124.62	136.15	10.53	150.09	21.04	13.69		

Where duplicate signals are given for a ^{13}C shift, these arise from the complexation of two distinct isomers [e.g., 4(b) C_3 114.02 and 114.50 ppm]. N/A, complex contains no acetate.

Table III ^{13}C-NMR Shifts of Various Adducts and Complexes (Given as δ ppm Relative To TMS)

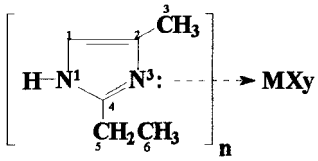

M = Zn, Ag ; X = Cl, NO_3

Complex	C_1	C_2	C_3	C_4	C_5	C_6
4a	119.50	128.15	10.47	149.76	20.76	12.87
		128.30				
5a	108.96	123.12	10.54	150.88	22.68	13.22
	113.91	133.74	10.97		24.04	14.00
EMI	116.68	130.52	11.65	148.24	21.41	12.87

Where duplicate signals are given for a ^{13}C shift, these arise from the complexation of two distinct isomers [e.g., 4(a) C_2 128.15 and 128.30 ppm].

UV-VIS Data

The UV-VIS spectroscopic data for the metal–imidazole complexes are given in Table V. It should be noted that complexes 1a–1d did not yield UV-VIS spectra, because all transitions are spin forbidden (see Laporte rule $\Delta s \neq 0$).[10] In complexes 2a and 2c, the ν_3 band is split into three, due to the number of transitions to doubly excited states that occur in the same region; these acquire some intensity by means of spin-orbit coupling.[10] This ν_3 band is of high intensity, from which it is inferred that $Co(EMI)_4Cl_2$, 2a, and $Co(PGE\text{-}EMI)_4Cl_2$, 2c, are both of tetrahedral geometry (this confirms the visual observations pertaining to structure commented on earlier in this section). In contrast, however, the ν_3 band in 2d, $Co(PGE\text{-}EMI)_4(CH_3COO^-)_2$ is not split; the inference being that the (PGE-EMI)–metal complex is perfectly symmetrical, due to a smaller field strength resulting from the steric bulk of the ligand.

Owing to the diamagnetic nature of both silver and zinc, UV-VIS measurements could not be made on these complexes. However, previous work by Barszcz et al.,[11] involving the preparation of Ag^+ complexes of imidazoles, has shown these complexes to exist as linear $[LAgL]_n^+$ species (where L = imidazole ligand). Elemental analysis (Table I) shows that the silver exists as 1 : 2 metal : ligand complexes, and the zinc as 1 : 2 metal : ligand complexes with acetate and as 1 : 4 metal : ligand complexes with chloride. ^{1}H-NMR measurements show downfield shifts on the addition of metals, indicating the existence of complexation.

Thermal Dissociation Data

It should be noted that the NMR probe has a maximum operating temperature of 145°C, and this limits the observation of dissociation temperatures to those occurring below this point when using this technique.[6a,6c] In most cases, complexes were observed to be only partially dissociated by this temperature (Table VI), although $Cu(PGE\text{-}EMI)_4(CH_3COO^-)_2$ and $Cu(PGE\text{-}EMI)_4Cl_2$ (from an earlier study) had undergone complete dissociation by 130°C, using the VT-NMR method. An interesting aspect concerns the Ni complex, 3a, which at low concentrations (in d_6-DMSO) underwent dissociation at around 65°C, but at higher concentrations underwent spontaneous dissociation at room temperature. This spontaneous dissociation is the result of the formation of a deep blue $Ni(DMSO)_6^{2+}$ $[NiCl_4]^{2-}$ complex species, which is reversible.[12]

Owing to the large number of oxidation and spin states and coordination geometries involved, a simple treatment of the data is difficult. However, some general trends can be observed. For example, increasing the number of PGE-EMI ligands coordinated about a copper atom causes a systematic decrease in the onset of dissociation (e.g., the 1 : 4 complex with chloride has dissociation temperature of 120°C and the 1 : 1 complex is >145°C). The increased steric bulk of the li-

Table IV Selected IR Data (4000–370 cm^{-1}) for Metal–Imidazole Complexes

Complex	N—H str. ν/cm^{-1}	Im Ring str. ν/cm^{-1}	C—C Skeletal str. ν/cm^{-1}	Anti-Sym OCO str. ν/cm^{-1}	Sym OCO str. ν/cm^{-1}	$\Delta\nu$ OCO	C═N str. ν/cm^{-1}	C—N def. ν/cm^{-1}	C—OH str. ν/cm^{-1}	C—H Out-of-Plane Bends ν/cm^{-1}	Ring def. of Im Ring ν/cm^{-1}
EMI	3100–2500	1604–1583(s)	—	—	—	—	—	1447(b)	—	746(s)	640(m)
PGE-EMI	—	—	1600–1599(s)	—	—	—	1496(s)	—	1245(s)	692(s), 755(s)	—
1a	3214(s)	1606–1584(s)	—	—	—	—	—	1456(b)	—	776(s), 811(s)	639(s)
1b	3150(s)	1651	—	1568–1578	1435–1418	164	—		—	672(w), 739(w)	640
1c	—	—	1600(b)	—	—	—	1498	—	1242	689(s), 753(s)	—
1d	—		1577(b)		1417(m)	—	1495(w)	—	1242(m)	693(s), 755(m)	—
2a	3147(m)	1615(m)	—	—	—	—	—	1456(s)	—	738(m), 796(m)	639(s)
2b	3149(s)	ca. 1600	—	1568–1578	1434–1403	145	—	1434(m)	—	677(s), 789(w)	640
2c	—	—	1598–1587(b)	—	—	—	1456(s)	—	1243(b)	691(s), 751(s)	—
2d	—	—	1599–1588(b)	1558	1386	172	1495(s)	—	1244(s)	692(s), 755(s)	—
3a	3217(s)	1609–1580(m)	—	—	—	—	—	1455(s)	—	777(s), 809(s)	639(s)
3b	3200–3100(s)	1614(s)	—	1540–1520	1418	112	—		—	723(w), 742(w)	—
3c	—	—	1599(s)	—	—	—	1500–1490	—	1240(s)	691 753	—
3d	—	—	1596–1588(b)	1546(w)	1430	116	1498	—	1244(s)	691 755	—
4a	3100–3000(b)	1615(m)	—	—	—	—	—	1456(s)	—	739(s), 776(s)	639(s)
4b	—	—	1600(m)	—	—	—	1498(s)	—	1242(s)	691(s), 753(s)	—
4c	—	—	1606(b)	—	1392(w)	—	1492	—	1241(s)	691(s), 753(s)	—
5a	3138(b)	1610–1588(m)	—	—	—	—	—		—	755(s), 692(s)	
5b	—	—	1588–1600(m)	—	—	—	1497–1337	—	1245(b)	693(s), 756(s)	—
5c	—	—	1599–1567(s)		—	—	1496–1402	—	1245(m)	693(s), 756(s)	—
6a	—	—	1599(b)–1600(b)	—	—	—	1497(s)	—	1245(s)	692(s), 755(s)	—
6b	—	—	1588–1600(m)	—	—	—	1493–1368(m)	—	1244(m)	693(s), 756(s)	—
6c	—	—	1588–1601(m)	1627	1430	197	1499(m)	—	1249(s)	692(s), 752(s)	—
6d	—	—	1561–1600(m)	1600	1390–1475	168	1492(m)	—	1245(s)	692(s), 756(s)	—
6e	—	—	1587(b)		1394–1436(b)	—	1494(w)	—	1245(s)	692(s), 756(s)	—

b, broad; m, medium; s, strong; w, weak

Table V UV/Visible Data (96% Ethanol) at 298 K

Complex	λ max/nm (ε/dm^3 mol^{-1} cm^{-1})	Ligand
1a		EMI
1b		EMI
1c	All transitions are spin forbidden	PGE-EMI
1d		PGE-EMI
2a	ν_1 = >900; ν_2 = 800; ν_3 = 566.6 (S), 594.5, 612.4 (I)	EMI
2b	ν_1 = >900; ν_2 = 800; ν_3 = 541.6, 563.2 (I)	EMI
2c	ν_1 = >900; no ν_2 observed; ν_3 = 584.2 (S), 618.0 (I), 635.6 (S)	PGE-EMI
2d	ν_1 = >900; no ν_2 observed; ν_3 = 565.1 (I)	PGE-EMI
3a	ν_1 = >900; ν_2 = 680.5, 736.6; ν_3 = 416.8	EMI
3b	ν_1 = 893.8; ν_2 = 684.0, 742; ν_3 = 402.1	EMI
3c	ν_1 = >900; ν_2 = 500–650 (B); ν_3 = 400–450 (B)	PGE-EMI
3d	ν_1 = >900; no ν_2 observed; ν_3 = 381.6 (B)	PGE-EMI
6a	ν_1 = 707.6	PGE-EMI
6b	ν_1 = 638.6, 660.1	PGE-EMI
6c	ν_1 = 748.0 (I); ν_3 = 370.0	PGE-EMI
6d	ν_1 = 754.8 (I); ν_3 = 370.0	PGE-EMI
6e	ν_1 = 675.3 (B); no band near 370 nm	PGE-EMI

I, intense; S, shoulder; B, broad.

gand contributes to the decreased stability of the resulting complex. There is also a trend observed on changing the anion in the copper series where substitution of chloride by nitrate causes an increase in dissociation temperature of 10°C. This is consistent with the position of these anions in the spectrochemical series. Interestingly, this effect of substitution on thermal stability is also ob-

Table VI Thermal Dissociation of Metal Complexes Containing PGE-EMI as a Ligand

Complex No.	Metal/Ligand Ratio	Thermal Dissociation Onset Temperature (°C)	Observed Color Changes as a Result of Dissociation
1c	1 : 3	>145	Orange/brown to yellow
1d	1 : 1	130	Light–dark brown
2c	1 : 4	105	Remained royal blue
2d	1 : 4	95	Violet to burgundy
3c	1 : 2	At low conc. ca. 65; at high conc. immediately at RT	Light blue to deep royal blue
3d	1 : 4	105	Green to yellow
4b	1 : 4	125	Cream to yellow/orange
4c	1 : 2	140	Straw to white ppt
5b	1 : 2	197[a]	No significant color changes
5c	1 : 2	140[b]	No significant color changes
6a	1 : 4.5	120	Dark green to amber
6b	1 : 4.5	130	Dark green to amber
6c	1 : 1	>145	Green khaki
6d	1 : 2	145	Blue to green
6e	1 : 4	115	Green to khaki

The NMR probe has a maximum operating temperature of 145°C, and this limits observation of the end of dissociation, unless otherwise stated.

[a] Complexes studied as solution of d_6-DMSO using 1,4-dimethoxybenzene as internal standard.

[b] Solid-state heating in vacuum oven.

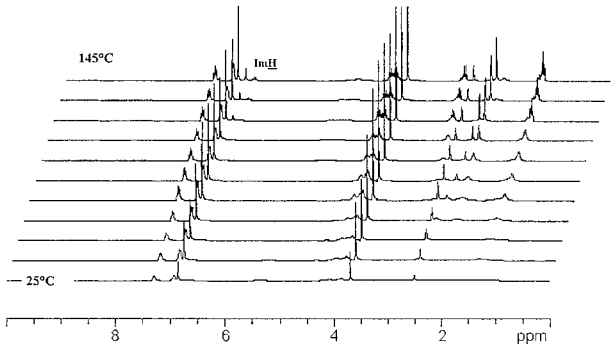

Figure 3 Stacked plot of 300 MHz ^{1}H-NMR of $Cu(PGE–EMI)_4(CH_3COO^-)_2$ in d_6-DMSO as a function of reaction time at 120°C.

served for the silver series (which was studied using TGA, because the dissociation temperature was above the maximum operating temperature of the NMR probe), where a difference of ca. 50°C is observed (in this case, upon substitution of acetate for nitrate). However, in this case the effect cannot be due to an orbital splitting effect since the silver is d^{10}. It should also be noted that while all of the chloride complex series showed reversible dissociation and recomplexation behavior, all of the corresponding acetates underwent dissociation followed by decomposition, making recomplexation impossible.

Kinetics of Cure as Monitored by ^{1}H-NMR Data

The proton designations referred to in this section are given in Figure 1. Figure 3 depicts a stacked plot for the progressive cure of a sample of commercial epoxy resin (Epikote 828) initiated with $Cu(PGE\text{-}EMI)_4(CH_3COO^-)_2$ (3 mol %) in d_6-DMSO at 120°C. In this curing reaction depicted schematically in Figure 2 protons H_c and H_d in the initial prepolymer (representing the oxirane ring) are shifted to new positions (H_c' and H_d', respectively) as cure proceeds and the environment of the protons changes. It is possible to resolve protons H_c, H_d, H_d' and H_a in the spectra. It can also be seen from Figure 3 that the integral of the oxirane protons decreases throughout the reaction as the oxirane ring is opened. The methyl protons H_a (of the isopropylidene bridging link) do not participate in the reaction, and so their chemical shift remains unchanged (and, hence, may be used as a reference signal in a quantitative ratio analysis).[6b] The concentration of epoxide was determined from the ratio of the signals from the protons of the oxirane ring and the protons of the isopropylidene group (which do not change throughout the course of the reaction). This provides two estimates of the concentration of the epoxide at each point in the reaction. The data used in this article are consistently taken from one of these estimates. The data for the complexes were treated in the same manner.

Solution Kinetics

Plots of ln[Epoxide] vs. time were used to determine the rates for the reactions. The rate constants being taken from the slopes of the best-fit lines by linear regression analysis. The correlation constants were typically 0.99. The data only showed evidence of a single slope, and could be interpreted in terms of an overall rate. The overall rate of reaction of the complexes with acetate as the counter ion, in solution are shown in Table VII. At the loadings indicated i.e., 3 mol % of the curing agent, Cu, Ni, and Co are of the same order of magnitude (10^{-4} s^{-1}). This is two orders of magnitude greater than that of the ligand alone (10^{-6} s^{-1}) at this temperature (Fig. 4). The kinetic data for the cobalt acetate complex (2d) are shown as Figure 5. The silver acetate complex (5c) and copper nitrate (6b) are also of the same order of magnitude. The slowest of the complexes is the silver complex with nitrate as the counter ion (5b). This may be due to the fact that silver forms polymeric species,[11] which are more difficult to dissociate. This is also shown by the dissociation temperature of the silver nitrate complex (5b), which is the highest at 197°C (measured by TGA). There is obviously a dependence on the counter ion with the acetates being generally faster than the nitrates. One would expect the electron-with-

Table VII ^{1}H-NMR Kinetic Data for Different Curing Agents at 120°C (in d_6-DMSO)

Curing Agent (3 mol % Incorporation)	k_2 Rate (s^{-1}) (Overall Rate)
$Cu(CH_3COO^-)_2(PGE\text{-}EMI)_4$	3.25×10^{-4}
$Ni(CH_3COO^-)_2(PGE\text{-}EMI)_4$	3.03×10^{-4}
$Co(CH_3COO^-)_2(PGE\text{-}EMI)_4$	1.93×10^{-4}
$Ag(CH_3COO^-)(PGE\text{-}EMI)_2$	7.65×10^{-5}
$Ag(NO_3^-)(PGE\text{-}EMI)_2$	8.33×10^{-6}
$Cu(NO_3^-)_2(PGE\text{-}EMI)_4$	5.50×10^{-5}
PGE-EMI	6.67×10^{-6}

k_2 refers to Figure 2.

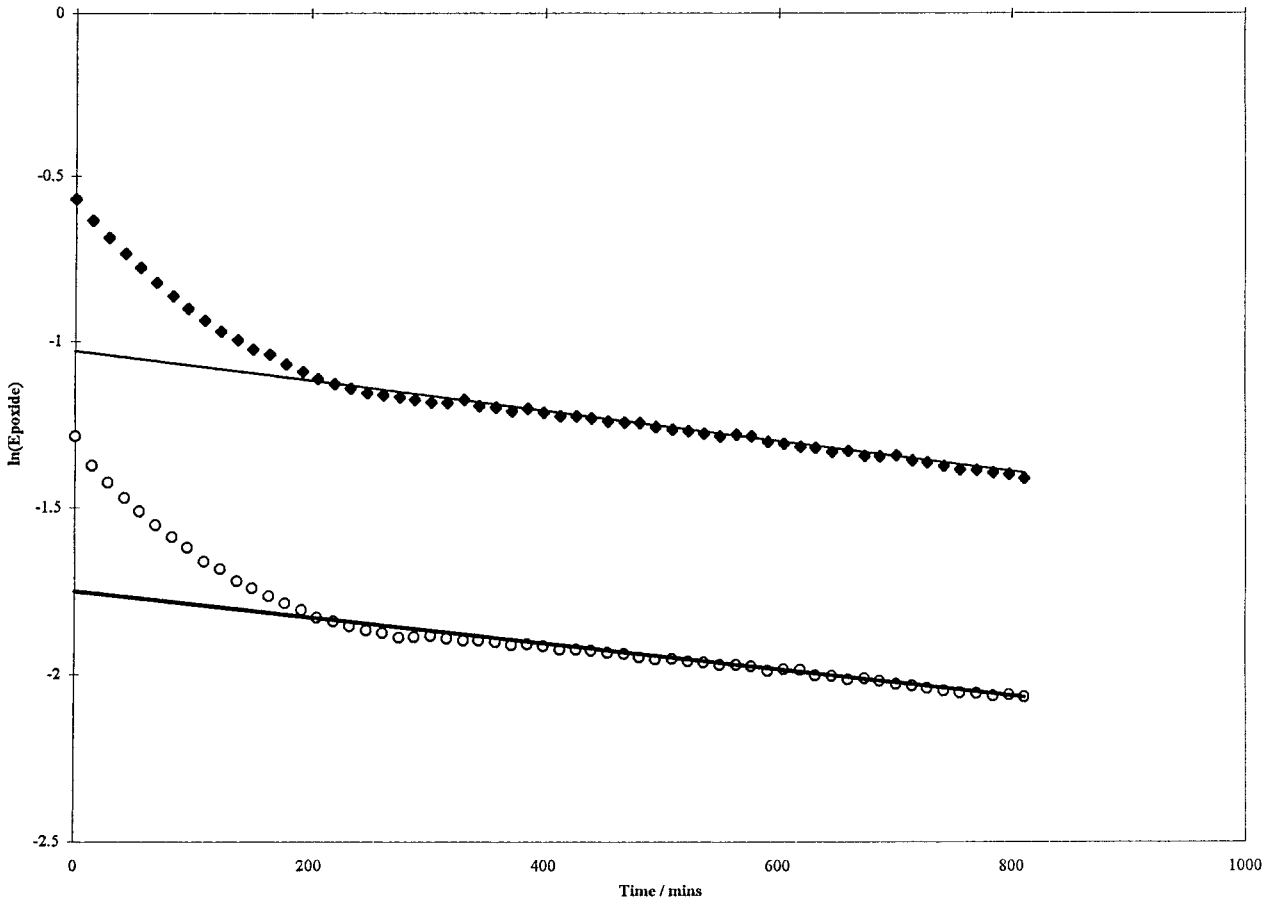

Figure 4 Plot of ln[Epoxide] vs. time (minutes) for Epikote 828 and PGE-EMI (3 mol %) in d_6-DMSO as a function of reaction time at 120°C (◆ = H_d/H_a; ○ = ln H_c/H_a; proton designations refer to Fig. 1).

drawing effect of the nitrate anion to stabilize the complex, and thereby reduce the rate of the reaction. The dissociation temperature of the copper nitrate complex (6b) is 130°C, and this is the second highest dissociation temperature and the second lowest of the rates of the complexes observed.

The order of the rate of reaction for the Cu, Ni, and Co complexes follows the Irving-Williams series of thermal stability and points to the stability of the complex as an important factor in their rates of reaction. Interestingly, the rate of reaction is proportional to the dissociation temperature in d_6-DMSO for these complexes. The copper complex (6e) dissociates at 115°C, the nickel complex (3d) at 105°C, and the cobalt (2d) at 95°C. The presence of the commercial epoxy, Epikote 828, reduces the stability of the complexes in solution accounting for the observed kinetic results.

Bulk Kinetics

Both the shape of the data plots and the reaction rates for the Cu, Ni, and Co complexes are different in the bulk at 120°C (Table III). There is a marked curvature in the plot of the initial data, indicating that there is a two-stage process occurring. Therefore, it is possible to derive two rate constants for this reaction, instead of the overall parameter for the solution studies. This curvature is also apparent in the reaction of the parent ligand alone with epoxy (Fig. 6), and probably represents the formation of the ring opened intermediate (Fig. 2). The nickel acetate complex (3d) (Fig. 7) is faster than the copper acetate complex (6e), both on adduct formation and subsequent reaction. The slowest complex is still the cobalt acetate complex (2d) the k_2 rate being an order of magnitude less. In fact, the rate of intermediate formation for the cobalt complex is only approxi-

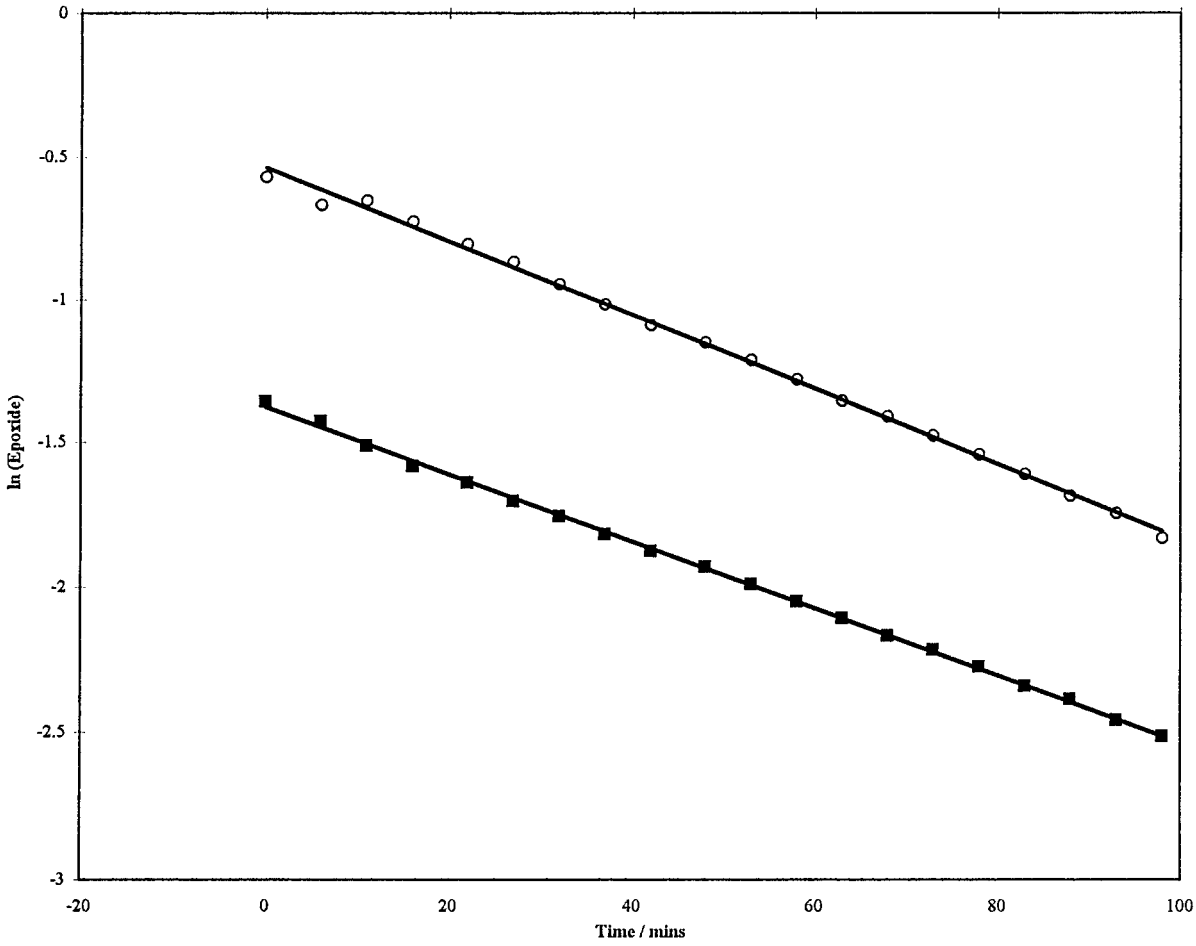

Figure 5 Plot of ln[Epoxide] vs. time (minutes) for Epikote 828 and Co(PGE–EMI)$_4$(CH_3COO^-)$_2$ (3 mol %) in d_6-DMSO at 120°C (○ = ln H_d/H_a; ■ = ln H_c/H_a; proton designations refer to Figure 1).

mately five times faster than that of the parent ligand.

CONCLUSIONS

The production of a wide range of complexes of EMI and PGE-EMI with 3d transition metals and silver and zinc with varying counter ions is shown to be feasible. However, there is a wide variation in the range of coordination geometries, spin states, and oxidation states. This variation makes the systematic understanding of the subsequent thermal dissociation of these complexes difficult, and further work is under way to prepare a more complete series of com-

Table VIII ^{1}H-NMR Kinetic Data for Different Curing Agents at 120°C (in Bulk)

Curing Agent (3 mol % Incorporation)	k_1 Rate (s^{-1}) (Adduct Formation)	k_2 Rate (s^{-1}) (Polyetherification)
Cu(CH_3COO^-)$_2$(PGE-EMI)$_4$	5.82×10^{-3}	1.08×10^{-4}
Ni(CH_3COO^-)$_2$(PGE-EMI)$_4$ [a]	5.95×10^{-3}	1.45×10^{-4}
Co(CH_3COO^-)$_2$(PGE-EMI)$_4$	4.97×10^{-3}	5.67×10^{-5}
PGE-EMI	5.18×10^{-3}	1.88×10^{-5}

k_1 and k_2 refer to Figure 2.
[a] Kinetic parameters calculated on data collected at 100°C.

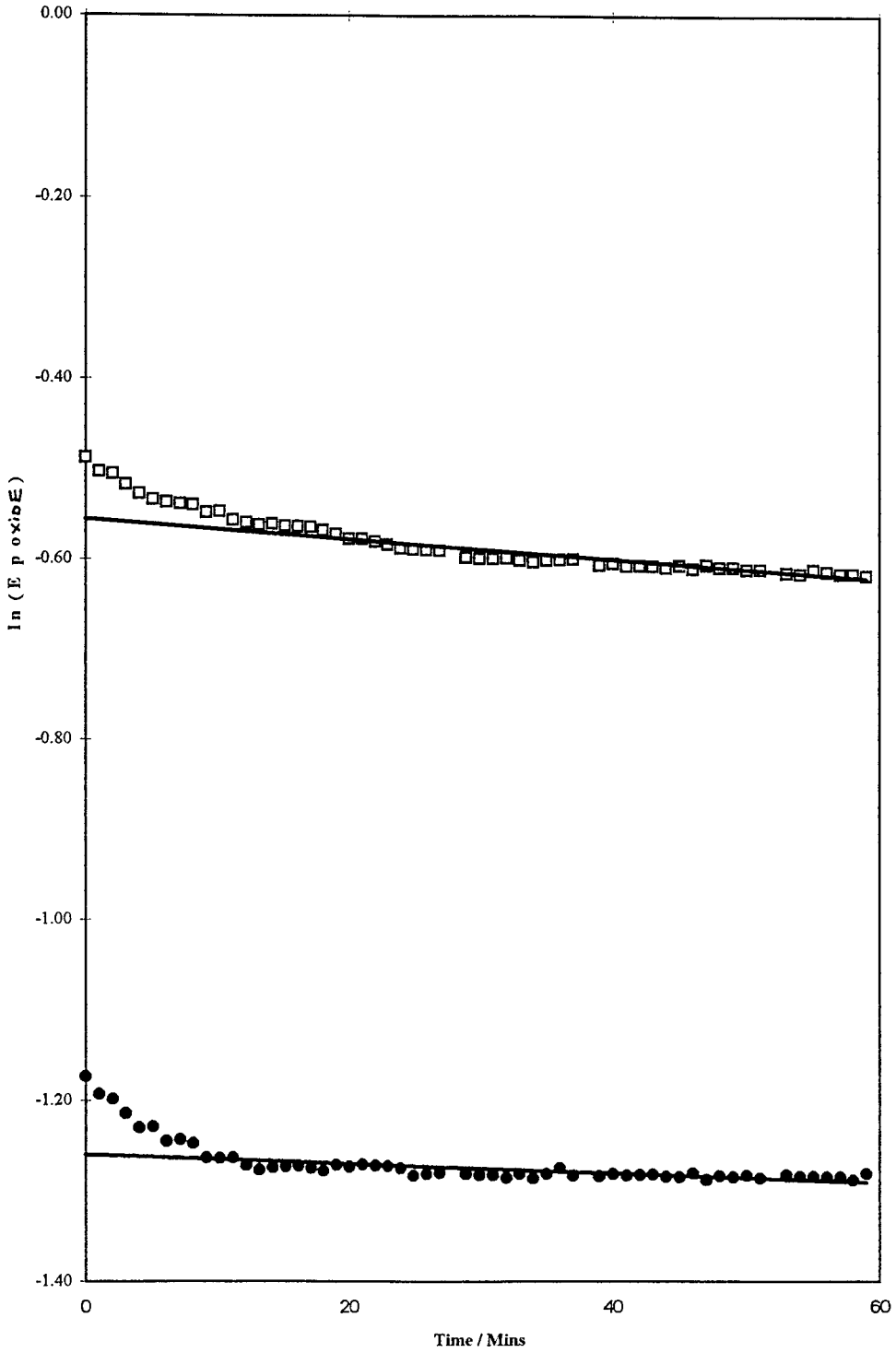

Figure 6 Plot of ln[Epoxide] vs. time (minutes) for Epikote 828 and (PGE–EMI) (3 mol %) at 120°C (bulk state) (□ = ln H_d/H_a; ● = ln H_c/H_a; proton designations refer to Fig. 1).

pounds. This, in turn, leads to complicate their use as latent curing agents for epoxy resins. Some general trends in dissociation temperature were noted, however, particularly the effect of changing the counter ion from chloride to nitrate. Even more striking is the effect of

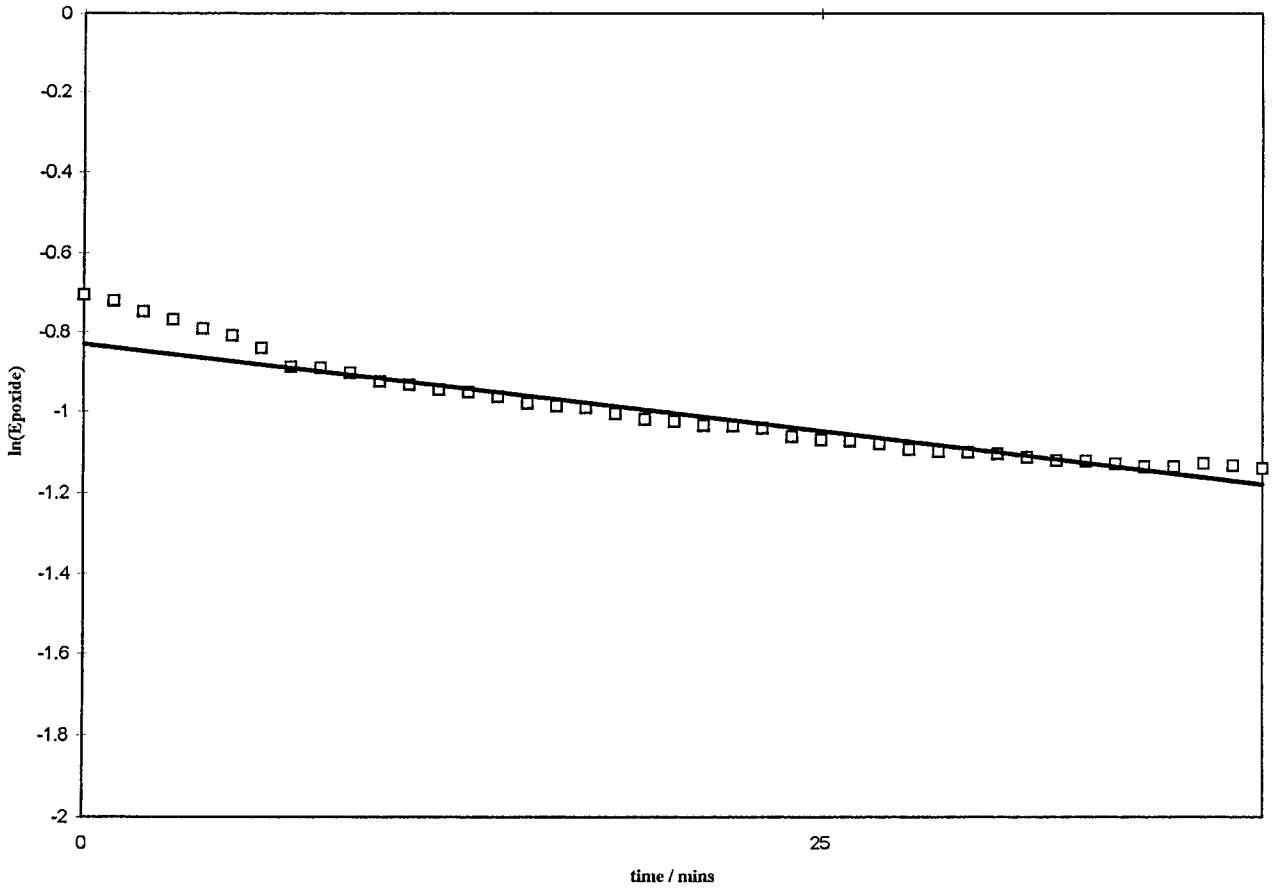

Figure 7 Plot of ln[Epoxide] vs. time (minutes) for Epikote 828 and Ni(PGE–EMI)$_4$(CH_3COO^-)$_2$ (3 mol %) at 100°C (bulk state) (□ = ln H_d/H_a; proton designations refer to Fig. 1).

changing the counter ion to acetate, which leads to irreversible dissociation.

We have investigated further the dissociation mechanism that causes the PGE-EMI ligand to be liberated, prior to initiating epoxy cure. We have shown that the thermal dissociation temperature is dependent on both the anion and transition metal in the complex. All of the complexes studied here have the ability to initiate the cure of a commercial epoxy resin via a polyetherification mechanism. For the first row transition metal elements there is a slight dependence on the nature of the metal atom (i.e., for the acetate series the nickel complex, 3d, and the copper complex, 6e, show approximately the same behaviour, whereas the cobalt complex, 2d is markedly different). The Co^{2+} cation is d^7 and the complex is low spin, and this may contribute an extra measure of stability. The acetates and nitrates are also markedly different, showing a dependence on the counter ion (i.e., the electron-withdrawing effect of the nitrate enhances the stability of the complex and reduces its reactivity). It should be noted that the acetate can also contribute to the initiation of the cure reaction, whereas the nitrate would not be expected to initiate cure in the same manner. These results may, in turn, provide a rationale for the development of a series of complexes with "tailorable" dissociation temperatures, depending on the particular anion and metal chosen.

This work was supported by Cookson Technology Group, Yarnton, on an EPSRC CASE studentship (J.B.). The authors wish to thank Ms. Izoldi P. Bezougli and Professor Mike Mingos of Imperial College, London, for the use of far-IR facilities; Ms. Nicola Walker for elemental analysis, and Mr. James P. Bloxsidge (both University of Surrey) for NMR analyses. The commercial epoxy (Epikote 828) was donated by Shell UK Ltd.

REFERENCES

1. Dowbenko, R.; Chang, W.; Anderson, C. C. U.S. Pat. 3,677,978, 1972.
2. Ito, M.; Hata, H.; Kamagata, K. J Appl Polym Sci 1987, 33, 1043; and refs. therein.
3. Jackson, R. J.; Pigneri, A. M.; Gaiogoci, E. C. SAMPE J 1987, 23, 16.
4. Dowbenko, R.; Chang, W.; Anderson, C. C. Ind Eng Chem Prod Res Dev 1971, 10, 344.
5. Barton, J. M. U.K. Pat. 2135316B, 1984.

6a. Barton, J. M.; Buist, G. J.; Hamerton, I.; Howlin, B. J.; Jones, J. R.; Liu, S. J Mater Chem 1994, 4, 379.

6b. Buist, G. J.; Hamerton, I.; Howlin, B. J.; Jones, J. R.; Liu, S.; Barton, J. M. J Mater Chem 1994, 4, 1793.

6c. Barton, J. M.; Buist, G. J.; Hamerton, I.; Howlin, B. J.; Jones, J. R.; Liu, S. Polym Bull 1994, 33, 215.

7. Poncipe, C. Ph.D. Thesis, University of Surrey, 1985.
8. (a) Hamerton, I.; Howlin, B. J.; Jones, J. R.; Lu, S.; Barton, J. M. J Mater Chem 1996, 6, 305; (b) Barton, J. M.; Hamerton, I.; Howlin, B. J.; Jones, J. R.; Lu, S. Polym Bull 1994, 33, 347; (c) Barton, J. M.; Hamerton, I.; Howlin, B. J.; Jones, J. R.; Lu, S. Polym Int 1996, 41, 159.
9. Eilbeck, W. J.; Holmes, F.; Taylor, C. E.; Underhill, A. E. J Chem Soc (A) 1968, 128.
10. Shriver, D. F.; Atkins, P. W.; Langford, C. H. Inorganic Chemistry; Oxford University Press: Oxford, 1990, p. 448.
11. Barszcz, B.; Gabryszewski, M.; Kulig, J.; Lenarcik, B. J Chem Soc Dalton Transact 1986, 10, 2025.
12. Meek, D. W.; Straub, D. K.; Drago, R. S. J Am Chem Soc 1960, 82, 6013.